Circulation rate modelling of mill charge using position emission particle tracking

ARTICLE *in* MINERALS ENGINEERING · FEBRUARY 2011

Impact Factor: 1.6 · DOI: 10.1016/j.mineng.2010.09.006

3 AUTHORS:

Daramy Kallon
University of Cape Town
1 PUBLICATION **3** CITATIONS
SEE PROFILE

Indresan Govender
University of KwaZulu-Natal
35 PUBLICATIONS **141** CITATIONS
SEE PROFILE

Aubrey Mainza
University of Cape Town
35 PUBLICATIONS **162** CITATIONS
SEE PROFILE

Minerals Engineering 24 (2011) 282–289

Contents lists available at ScienceDirect

Minerals Engineering

journal homepage: www.elsevier.com/locate/mineng

Circulation rate modelling of mill charge using position emission particle tracking

D.V.V. Kallon [a], I. Govender [a,b,*], A.N. Mainza [a]

[a] Center for Minerals Research, Department of Chemical Engineering, University of Cape Town, South Africa
[b] Department of Physics, University of Cape Town, South Africa

ARTICLE INFO

Article history:
Available online 13 December 2010

Keywords:
Circulation rate
PEPT
Charge features
Charge transitions

ABSTRACT

A model linking the circulation rate of charge particles with physical mill parameters (load fraction, shoulder angle and friction) has been developed and tested using experimental data derived from positron emission particle tracking (PEPT). The model parameters are obtained directly from the *in situ* flow field of the PEPT tracer particles. The model formulation, methodology for model parameter correlations and comparison of circulation rate model with direct measurement from PEPT forms the focus of this paper.

1. Introduction

One of the earliest works on charge motion was reported by White (1905), who assumed that particles along the mill periphery move without slip until a gravitational and centrifugal force balance is reached. At this stage particles are projected into parabolic motion, strike the "impact point" and are drawn into the bulk of the charge. His conclusions on regulating water levels in order to generate useful impact work are a valuable contribution to comminution. At the end of the next decade, Davis (1919) formulated a similar mathematical description for a single particle moving along the mill shell without slip. Verification of the theoretical results was achieved by taking end window images of an experimental mill. The agreement between experiment and theory was said to compare well except for the intersecting trajectory paths of cataracting particles observed in experiments. This was argued away as accidental and amplified by a low charge filling. His work clearly highlights the value of mathematical modelling of charge motion while elucidating the shortcomings of simplified assumptions.

Other notable contributions on charge motion analysis has been the development of grinding theories such as the energy distribution theory (Rittinger, 1867; Bond, 1952; Schonert, 1988) and the breakage theory of comminution (Kick, 1885; Powell and McBride, 2006). These dynamical theories would lead one to conclude that for a given feed material and energy input the best comminution device is one which could provide the correct fracture energy to each target product particle size distributions (PSDs), bearing in mind the advantage of power efficiency. Studies on liner designs (Mcler, 1983; Vermeulen, 1985; Vermeulen and Howat, 1988), illustrate the impact of these theories on comminution. Vermeulen and Howat (1988) suggested the charge surging phenomenon commonly encountered in smooth lined rod mills contributes to liner wear, because the large fluctuations in slip induced massive wear on the lining and clearly illustrated the value of using lifter bars.

Qualitative flow phenomena are not only describable from experiments but can also be reproduced through numerical simulations. These simulations are computationally intensive but are becoming more popular as computer processing power has increased. A range of techniques have recently been employed which vary from treating the material being studied as a continuum, with the physics averaged out over all the particles (Charles, 1957), through to treating each particle as a discrete element (Discrete Element Modelling – DEM), Powell and McBride (2006). An essential aspect of DEM simulations is that collision interaction of particles with each other and their environment are detected and modelled using contact force laws. Equations of motion are then solved for the particle motions and for the motion of any boundary objects with which the particles interact (Walton and Braun, 1993; Powell and McBride, 2006). Among the most recent studies undertaken using this technique includes a 142 mm laboratory tumbling mill (Powell and McBride, 2004; Govender, 2005). In these studies, a number of characteristics including charge behaviour, torque and power draw for a range of rotation rates (between 50% and 130% of the critical speed for mills) were analysed.

However, to date there is a notable lack of information on the actual trajectories followed by particles in rotary grinding mills. In particular the speed of circulation of the charge particles relative to the mill rotation, otherwise known as the circulation rate, has

* Corresponding author at: Department of Physics, University of Cape Town, South Africa. Tel.: +27 21 650 5554; fax: +27 21 021 650 3342.
E-mail address: indresan.govender@uct.ac.za (I. Govender).

0892-6875/$ - see front matter © 2010 Elsevier Ltd. All rights reserved.
doi:10.1016/j.mineng.2010.09.006

Nomenclature

a	charge acceleration	N_m	mill speed
C	circulation rate	n_l	number of rolling, cascading or cataracting layers from base of mill
C_r	circulation ratio		
CoC	centre of circulation	r	orbital radius
CoM	centre of mass	R	mill radius
D	degree of slip	v	tangential velocity of mill
d_m	mean particle diameter	ω	angular velocity
F_c	centrifugal force	α	load fraction
F_F	frictional force	δ	angle of repose
F_g	force of gravity	θ	dynamic angle of repose
F_N	normal force caused by friction	θ_c	critical angle of repose
F_r	Fraude number	ζ	departure shoulder angle
f	filling degree	ε	filling angle
g	acceleration due to gravity	μ_i	internal friction coefficient
k_m	mean charge deflection	μ_w	wall friction coefficient
N_c	critical mill speed	μ_k	coefficient of kinetic friction

never been directly investigated and as such is often taken to be unity by many mill models. This apparently is to allow for simple mathematical manipulation of these models.

A comminution device is equipment that converts an input of energy into mechanical motion. This motion is transferred to the content of the device – charge – and the resultant mechanical action applied to the particles leads to their damage and eventual breakage (Powell and McBride, 2006). In this paper, we discuss recent work done on charge motion analysis from an *in situ* perspective using data derived from the novel positron emission particle tracking (PEPT) technique. New descriptions of the transition behaviour between the main forms of motion, as previously investigated by Mellmann (2001), is presented and used in formulating a mathematical model of circulation rate which is well supported by PEPT data.

2. Experimental work

The data used in this research is derived from the experimental program conducted by the Centre for Minerals Research (University of Cape Town) at the PEPT centre of the University of Birmingham (UB). The data derived from the particle tracking system spans a wide range of dry and wet milling configurations and a number of experiments have been conducted over a period of 3 years. Traditional autogenous and semi-autogenous mills were employed mostly in closed circuits and a detailed summary of these experiments is presented herein.

The experimental rig, Fig. 1, consisted of a mill constructed from High Density Polyethylene (HDPE), a DC drive with step-down gear box, torque sensor and a reticulating pump for wet experiments that re-circulated the slurry. The details of the mill are as follows: internal length of 270 mm, internal diameter 300 mm, number of lifters 20, and discharge grate open area ~30%. The mill shell, the lifters and the pulp lifters are manufactured from HDPE which has a specific density of 0.95. HDPE is chosen specifically for this type of experiment because of its low gamma ray attenuation. The grate and the mill cover are manufactured from clear acrylic, so that the discharge dynamics of the mill can be observed using video and photographic cameras. Milling configurations spanned six lifter profiles, five loads between 12.5% and 50% and five speeds between 55% and 100% of critical. The effective grinding length (EGL) is the same as the internal length of the mill for all loads since the mill is flat ended.

3. Charge motion at low speeds – the centre of circulation (CoC) model

The centre of circulation (CoC) is a unique point about which the entire charge appears to circulate as distinguished from the mill centre. The path of the particles in the *en-masse* region form concentric rings of decreasing radii that converge on the CoC. If the circulation plane of the mill is divided into families of horizontal, vertical and radial control surfaces, a cumulative count of particles passing through any point along these control surfaces would yield a local maximum when the particles pass through the CoC (Powell and McBride, 2004). According to Powell and Nurick (1996), the radial and angular positions of the CoC are determined by the instantaneous charge position which in turn is influenced by the mill rotational speed. The initial radial and angular locations of the CoC are observed when the first layer of balls roll down the charge surface. There is a notable initial outward shift of the CoC as more underlying layers enter rolling motion with a corresponding drop in its angular location. At higher speeds, however, this trend is reversed, the CoC tends towards the mill centre and its angular position climbs rapidly towards 90°. A mathematical model, given in Eq. (1), describes the radial displacement of the CoC at low speeds.

$$r_{CoC} = n_l d_m + R\sqrt{1-\alpha} \tag{1}$$

According to Watanabe (1999), the radial position of the charge surface for a mill at rest is given by $R\sqrt{1-\alpha}$. For a mean particle diameter d_m, n_l would represent the number of particle layers leaving the base of the mill and entering rolling, cascading or cataracting motion. This phenomenon is illustrated in Fig. 2a. For a given maximum radial location of the CoC (Fig. 2a) the outward shift of the CoC ($r_{CoC(max)} - r_{CoC(initial)}$) increase with mill load fraction indicating the possible use of the CoC model for an analysis of charge slippage – which is out of scope of this paper.

In comminution the angle of repose is commonly employed in describing the torque exerted by the charge, and consequently the power drawn. Powell and McBride (2004) have presented the most user-independent definition for the repose angle by noting that "the tangent to the equilibrium surface at the CoC is perpendicular to the radial line passing through the CoC. This condition is uniquely defined because the equilibrium surface has a different curvature to the mill shell, so only one point on the surface can have a tangent perpendicular to a radial line".

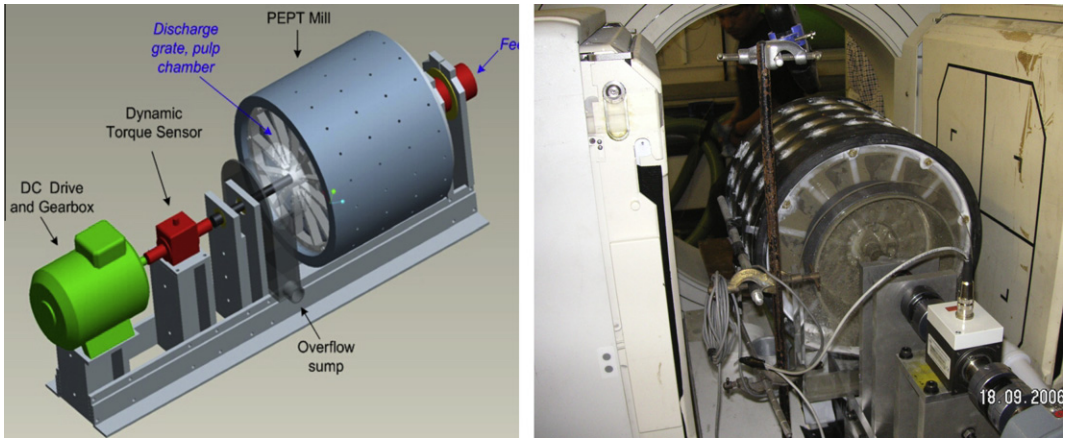

Fig. 1. Experimental mill employed in positron emission particle tracking experiments. The right image illustrates the mill between the two detectors of the PEPT camera.

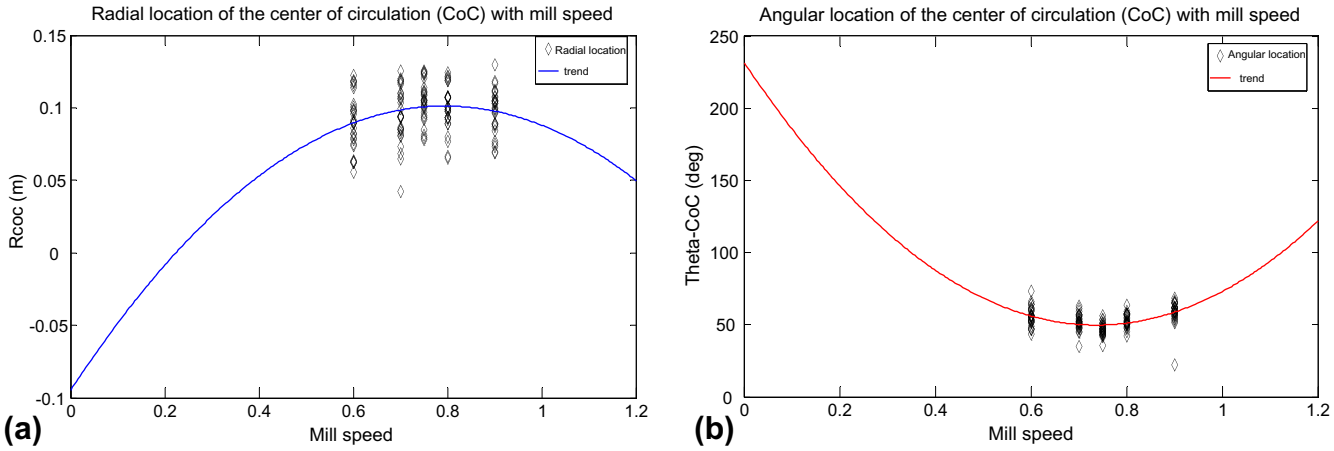

Fig. 2. Variation of radial and angular positions of the centre of circulation (CoC) with mill speed.

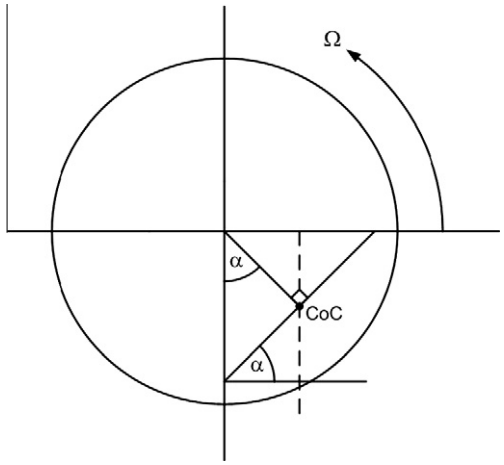

Fig. 3. Illustration of the angle of repose redrawn from Govender (2005).

According to Govender (2005), closer inspection of the geometric implications of the Powell and McBride definition (2004), reveal that the angle of natural repose is simply the angular position of the CoC, Fig. 3. Fig. 2b indicates that this angle tends towards 90° as the CoC approaches the mill centre (Powell and Nurick, 1996).

4. The toe and shoulder (TaS) – the charge repose

The importance of the toe and shoulder in comminution research can hardly be overstated. Some researchers have used their definitions to provide a description of the angle of repose of mills as the line joining the toe and shoulder of the charge (Rolf and Vongluekiet, 1984; Liddell and Moys, 1988; Yashima et al., 1988; Fuerstenau et al., 1990). Recent work by Powell and McBride (2004), has revealed the inherent shortcomings of these eye-balled definitions since they cannot hold true at speeds greater than 80% of the critical. They proposed the concept of a departure and head shoulder in describing a shoulder region and an impact and bulk toe for the toe region.

According to these authors (Powell and McBride, 2004), the departure shoulder (DS) is defined as the uppermost point at which the charge departs from the shell of the mill. The media may still travel along the surface of a lifter bar, or may still be travelling in an upwards direction, prior to entering cascading/cataracting motion. The head shoulder (HS) is defined as the apex position reached by the charge, so it is the highest vertical position that the charge attains. The bulk toe (BT) is located by the point where the horizontal extension of the horizontal equilibrium surface from the inflection point (defined as the point at which the horizontal equilibrium surface moves in an upwards direction towards the impact toe) intersects the shell. The impact toe (IT) is where the cataracting charge impacts the shell in the toe region when the speed is sufficiently high. This is given by the point

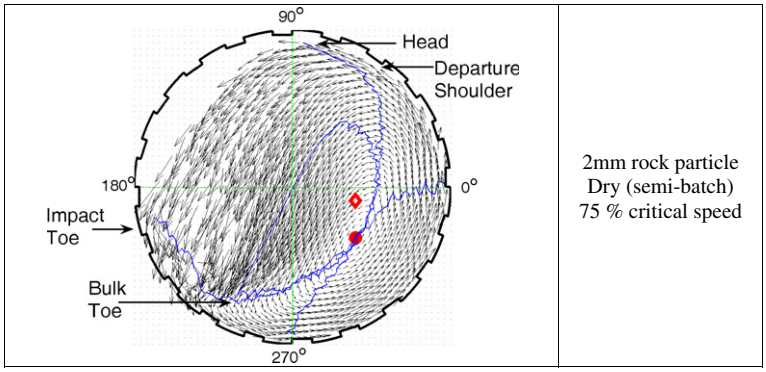

Fig. 4. Identifying the toe and shoulder regions. The 'blob' indicates the CoC while the 'diamond' identifies the centre of mass.

where the horizontal equilibrium surface intersects the shell of the mill in the toe region, Fig. 4. The angle formed (at the mill centre) by a line joining the points where the charge in the *en-masse* region is in initial and final contact with the mill taken in the direction of the mill rotation is the charge repose. In other words it is the angle at the mill centre formed by a line joining the impact toe and the departure shoulder.

4.1. Two important transition behaviours

Grinding media motion ranges from a slipping bed that appears to be stationary (Vermeulen and Howat, 1988; Mellmann, 2001), to a bed that sticks to the shell and rotates with the mill (Watanabe, 1999). Between these two states motion is principally categorized into three main forms and seven subtypes as illustrated in Table 1.

Several authors (White, 1905; Mcler, 1983; Vermeulen, 1985; Vermeulen and Howat, 1986, 1988; Schonert, 1988; Mellmann, 2001; Powell and McBride, 2004; Govender, 2005) have given clear descriptions of these motion categories and their subtypes developing mathematical models with varying degrees of validity. Here we look at transition behaviour between the three main categories, that is, from slipping to cascading and from cascading to cataracting.

4.1.1. Slipping to cascading transition – the mill internal wall friction model

Mellmann (2001) published a detailed investigation of charge motion transition behaviour from slipping to cascading deriving a dependency on the mill critical wall friction coefficient, Eq. (2). He showed this wall friction coefficient (μ_w) to be determined by the filling angle (ε), the Froude number (F_r) and δ is the repose angle, Fig. 5.

$$\mu_w > \frac{2\sin^3\varepsilon\sin\delta}{3(1+F_r)(\varepsilon-\sin\varepsilon\cos\varepsilon)} \tag{2}$$

According to Mellmann (2001), with the onset of cascading motion a dynamic angle of repose (θ) which determines the new position of the centre of gravity of the charge is brought into play giving a critical wall friction coefficient shown in Eq. (3), where f is the filling degree.

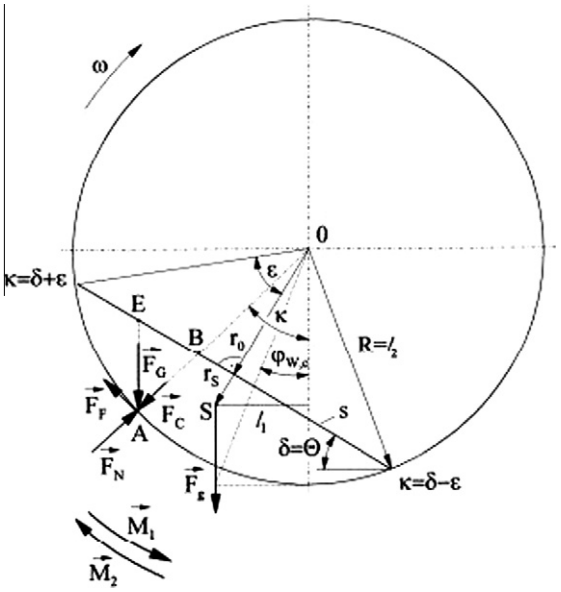

Fig. 5. Illustration of the mill geometry at low speeds – Mellmann (2001).

$$\mu_{\omega_c} = \frac{2\sin^3\varepsilon\sin\theta}{3\pi f(1+F_r)} \tag{3}$$

On closer analysis we have found Eqs. (2) and (3) to be valid only for low speeds due to their dependence on over-simplified charge geometry. For a mill with a size distribution of particles running at higher speeds we present a new derivation herein. Our approach has shown that the transition condition can be written in terms of the polar coordinates of the centre of mass, the mean deflection of the entire charge from its initial position of rest and the tangential velocity of the mill – parameters readily measurable from the *in situ* flow fields of the PEPT tracer particle.

For moment balance around the axis of rotation, Fig. 5, let M_1 be the moment due to the gravitational pull (F_g) on the charge acting through the centre of mass (CoM) and M_2 moment due to frictional forces acting at the mill wall.

Table 1
Motion forms and their subdivisions.

Circular charge motion							
Forms	Slipping		Cascading			Cataracting	
Characteristics	Low friction and mill speeds		Sufficient friction and moderate speeds			Sufficiently high friction and very rigorous speeds	
Types	Sliding	Surging	Slumping	Rolling	Cascading	Cataracting	Centrifuging

Then for M_1:

- determine the centre of mass of the system, see Powell and Nurick, (1996), Govender (2005),
- calculate $F_{g,}$
- multiply F_g by l_1 the perpendicular length from mill centre (O) expressed in terms of r_i and θ_i the polar coordinates of the centre of mass (CoM),

i.e.

$$l_1 = r_i \sin\theta_i \tag{4}$$

Thus

$$M_1 = mgr_i \sin\theta_i \tag{5}$$

Similarly for moment caused by the wall internal friction M_2, let k_m be the mean charge deflection, $l_2 = R$, $F_G = mg$, $F_c = m\omega^2 R$, v is the mill tangential velocity.

- determine the mean deflection (k_m) of the charge from its initial resting position,
- calculate F_F the mean frictional force acting through the point of mean deflection (k_m) of the charge along the mill wall,
- multiply F_F by l_2 the perpendicular length from mill centre (O) equal to the mill radius in this case.

The normal force at mill wall:

$$F_N = F_G \cos k_m + F_c \tag{6}$$

becomes

$$F_N = mg \cos k_m + m\omega^2 R \tag{7}$$

Since

We then obtain

$$F_N = \mu_\omega (mg \cos k_m + m\omega^2 R) \tag{9}$$

which gives a moment at the mill wall of

$$M_2 = \mu_\omega m(Rg \cos k_m + v^2) \tag{10}$$

The transition to cascading occurs when the moment at the mill wall caused by friction overcomes the effect of gravity (Mellmann, 2001).

$$M_2 > M_1 \tag{11}$$

Giving a limiting coefficient of friction of:

$$\mu_\omega > \frac{gr_i \sin\theta_i}{(Rg \cos k_m + v^2)} \tag{12}$$

Eq. (11) shows that the transition condition to cascading can be independent of the mass of the assembly and the ranges of Froude number, and hence independent of bed material used. The relationship between wall friction coefficient and mill speed is shown in Fig. 6 below. This graph (Fig. 6) shows the rapidly declining effect of friction on the circulating particles as mill speed is increased, becoming zero at approximately 96% critical speed. Beyond this point the charge is centrifuged entirely under the effect of centrifugal forces. The mean charge deflection k_m is the mathematic mean of media positions along the mill periphery a time (t) or half the charge repose. This angle coincides with the 270° line at only two instances of charge motion: at time (t_0) and at total centrifuging, giving $\cos k_m = 0$. Furthermore assuming a uniform distribution of particles at time (t_0) the angular location of the CoM will coincide with this line giving $\sin\theta_i = -1$. Hence the maximum attainable friction occurs at mill start up (i.e. at time t_0) and is given by Eq. (12). The initial tangential acceleration of the centre of mass $a_{CoM(i)}$ would be the same as the mill acceleration for the charge and mill to move together as one rigid body – important to industrial applications. The negative sign in Eq. (12) is well supported by the graph in Fig. 6.

$$\mu_{\omega(\max)} = \frac{-gr_{CoM(i)}}{v^2} = -\frac{g}{a_{CoM(i)}} \tag{13}$$

4.1.2. Cascading to cataracting transition – the mill speed model

Cataracting motion, prominently encountered in industrial tumbling mill operations, is characterized by free flight – a trajectory starting with particle throw-off at the departure shoulder and ending with impact at the toe region. Mellmann (2001) suggested radial equilibrium of forces at the mill wall would yield a line of detachment that obeys a circle through the axis of rotation. This circle is known as the Davis circle (see Davis, 1919), with diameter g/ω^2 as illustrated in Fig. 8. The line OP_2 is a logarithmic line providing a transition to cataracting according to Eq. (13), (Mellmann, 2001).

$$F_r = \frac{\omega^2 r}{g} > \sin\zeta \tag{14}$$

where r is the orbital radius as shown in Fig. 8 below. However, since the mill rotational speed induces motion in grinding media we found it necessary to investigate this transition phenomenon in terms of the speed required to project a particle at point P_2 into

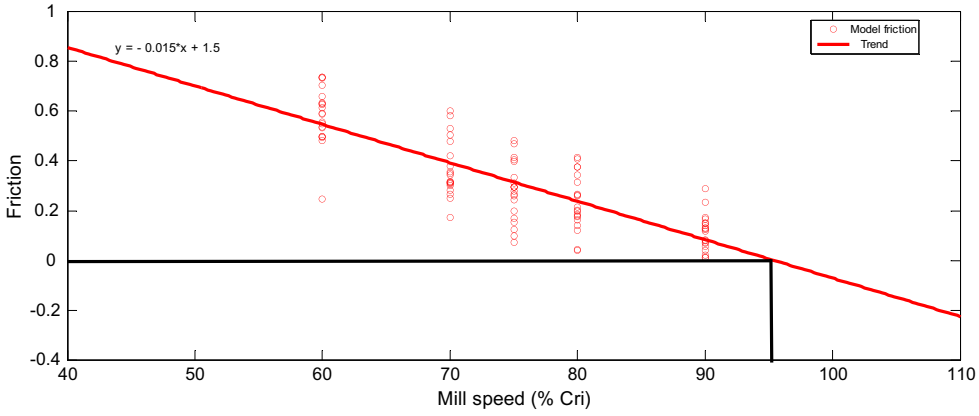

Fig. 6. Wall friction coefficient versus mill speed.

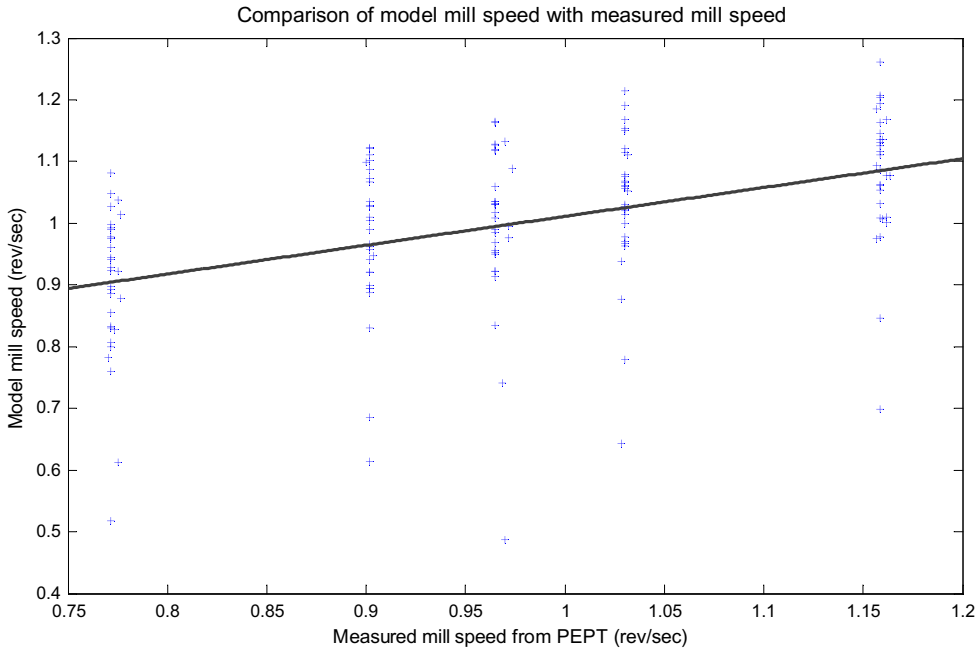

Fig. 7. Comparing model and experimental mill speeds.

cataracting. From the investigations of Watanabe (1999), we have developed a simplified model of mill speed that would, at a certain point, yield the critical rotation speed suggested by Watanabe (1999).

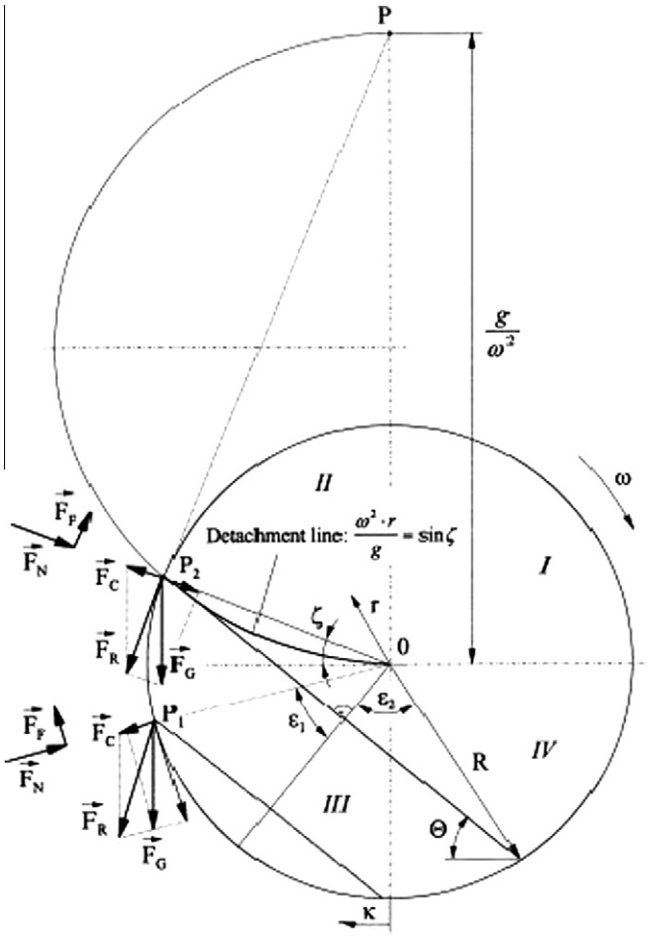

Fig. 8. Illustration of the mill geometry at high speeds showing the Davis circle – Mellmann (2001).

$$N_m = \frac{1}{2\pi}\sqrt{\frac{g\sin\zeta}{R\sin\theta_c\sqrt{1-\alpha}}} \tag{15}$$

N_m is the mill speed at the departure shoulder, θ_c the critical angle of repose. Eq. (14) shows the mill speed can be a function of the angle ζ at the point of detachment or departure shoulder and once this speed is exceeded particles are observed to deviate from the mill profile but may remain in an upward climb towards the head shoulder. Fig. 7 shows a close comparison between speeds used in PEPT experiments and those obtained from the model calculations (Eq. (14)).

According to Powell and Nurick (1996), the critical angle of repose for mills occurs at the point of total centrifuging and is equal to 90° since the CoC coincides with the mill centre at this stage. Accordingly, the numerator under the root sign in Eq. (14) will correspond to the mill centripetal acceleration acting along the line of detachment. Hence $g\sin\zeta = g$ at only one point along the mill profile, when $\zeta = 90°$ giving the original expression derived by Watanabe (1999). Clearly Watanabe's model is a special case since it is only valid at the point of total centrifuging while the model (in Eq. (14)) can be regarded as the mill speed whose effect, at declining wall friction coefficient, would cause the charge to tend towards the point of centrifuging.

5. A circulation rate model for the tumbling mill

Powell and McBride (2004), developed a scheme for calculating the circulation rate from knowledge of the centre of circulation (CoC) of the charge. The development of a numerical scheme by Govender et al. (2004), for validating DEM using PEPT data has shown that circulation rate can have a linear relationship with typical speeds encountered in industrial tumbling mill operations. Here we present a mathematical model that links circulation rate with mill speed and wall internal friction coefficient, Eq. (16).

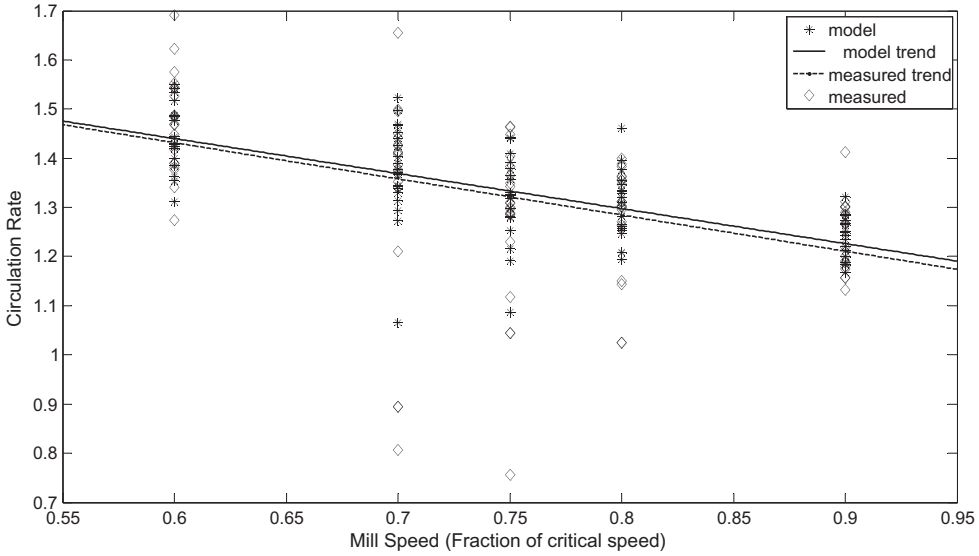

Fig. 9. Comparison of model circulation rate (Eq. (17)) with circulation rate obtained from PEPT experiments.

$$\text{Circulation rate } (C) = \text{friction coefficient } (\mu_k) + \text{mill speed } (N_m) \tag{16}$$

$$C = \tan\theta_{mean} + \frac{1}{2\pi}\sqrt{\frac{g\sin\zeta}{R\sin\theta_c\sqrt{1-\alpha}}} \tag{17}$$

where θ_{mean} is the mean angle of repose, $\mu_k = \tan(\theta_{mean})$ the coefficient of kinetic friction. Here we note that the model describes two distinct phases of charge motion which we have termed the slumping and cataracting cycles. During the slumping cycle successive avalanches at the surface causes the charge to oscillate about a mean deflection. The perpendicular to this mean deflection, taken at the charge surface, defines a line of static equilibrium achievable only when the coefficient of kinetic friction equals the tangent of the repose angle (Mellmann, 2001; Govender, 2005). This condition is unique and affected principally by friction at the mill wall and to a degree by the speed at which the mill is run. At a given wall friction coefficient, an increase in mill speed leads to a substantial accumulation of slumped layers causing the charge to level out into a flat bed surface (Powell and Nurick, 1995; Mellmann, 2001). When the first layer of balls roll down this surface the CoC assumes its initial location and the charge is essentially circulating. However, as Fig. 6 shows, the influence of friction on the circulating particles continue up to very high speeds. The cataracting cycle describes the circulation of the media around the CoC and range from rolling to total centrifuging, see Table 1.

The trajectory data of the tracked particle is used to determine the experimental circulation rate and the trend line so obtained is compared to the evaluated model circulation rate, Fig. 9. The results compare well for the range of speed and milling configurations used in this study. However, the second part of the expression in Eq. (16) would appear to be undefined in the lower quadrants. This essentially indicates that $g\sin(\zeta)$ would be a centrifugal acceleration – the reverse effect to the upper quadrants. Introducing a circulation ratio (C_r), Eq. (17), will yield a value of unity only when the mill speed is very high, see Fig. 6. At any speed below this point the charge would be expected to circulate faster than the mill rotation.

$$C_r = \frac{C}{N_m} = \frac{\mu_\kappa}{N_m} + 1 \tag{18}$$

6. Conclusion

A circulation rate model is proposed that integrates key features of charge motion in grinding media mills. The principal determinants are the speed at which the mill is run and the internal design of the mill which transfers mechanical energy to the charge in the form of rotational motion. For the range of speeds, loads and particle sizes used in this study the model correlates well with PEPT experimental data. Some of the most important findings were:

1. The rate of circulation of mill media can be expressed as a function of measurable mill operating parameters such as mill rotational speed, load fraction, charge natural angle of repose, departure shoulder angle and coefficient of friction depicting near linear trends.
2. While the rate of circulation of the charge was found to decrease with increasing mill speed, departure shoulder angle and load fraction, it increased with increasing wall friction coefficient illustrating the influence of liner designs on circulation rates.
3. There was no perfectly keyed-in motion, even for the outermost layer of the charge and all layers of the charge, irrespective of the speed and lifter configurations, were found to slip relative to the mill.
4. Experimental results showed clear cascading motion at 60%, cataracting at 75% and partial centrifuging at 90% of the critical speed.
5. The circulation rate of the media was found to be a maximum once the CoC was correctly located but there was no observable trend between circulation rate and the CoM. Accurate determination of the charge geometric location is dependent on the angular location of the CoC – natural angle of repose – and the charge repose – the line joining the impact toe and departure shoulder. Eqs. (1) and (12) show these features can have near linear relationships with industrial mill operating speeds.

Acknowledgements

Anglo Platinum for funding this research. Positron Imaging Centre at the University of Birmingham for use of the PEPT facility.

References

Bond, F.C., 1952. The third theory of comminution. Mining Engineering 4, 484–494.

Charles, R.J., 1957. Energy–size reduction relationship in comminution. Transactions of AIME Minerals Engineering 208, 80–88.

Davis, E.W., 1919. Fine crushing in ball mills. AIME Transactions 61, 250–296.

Fuerstenau, D.W., Kapur, P.C., Velamakanni, B.A., 1990. A multi-torque model for the effects of dispersants and slurry viscosity on ball milling. International Journal of Mineral Processing 28, 81–98.

Govender, I., 2005. X-ray Motion Analysis of Charge Particles in a Laboratory Mill. PhD Thesis, Dept. of Mechanical Engineering, University of Cape Town.

Govender, I., McBride, A.T., Powell, M.S., 2004. Improved experimental tracking techniques for validating discrete element method simulations of tumbling mills. Journal of Experimental Mechanics 14 (10), 153–160.

Kick, F., 1885. Das gasetz der proportionlen wilderstande und seine anwendung. Leipzig.

Liddell, K.S., Moys, M.H., 1988. The effects of mill speed and filling on the behaviour of the load in a rotary grinding mill. JSA Institute of Mining and Metallurgy 88, 49–57.

Mcler, R.E., 1983. Effects of speed and liner configuration on ball mill performance. Mining Engineering, pp. 617–622.

Mellmann, J., 2001. The transverse motion of solids in rotating cylinders – forms of motion and transition behaviour. Powder Technology 118, 251–270.

Powell, M.S., McBride, A.T., 2004. A three-dimensional analysis of media motion and grinding regions in mills. Minerals Engineering 17 (11), 1099–1109.

Powell, M.S., Mcbride, A.T., 2006. What is required from DEM simulations to model breakage in mills. Minerals Engineering 19, 1013–1021.

Powell, M.S., Nurick, G.N., 1996. A Study of charge motion in rotary mills: extension of the theory. Minerals Engineering 9 (2), 259–268.

Rittinger, P.R., 1867. Lehrbuch der aufbereitungskunde. Berlin.

Rolf, L., Vongluekiet, T., 1984. Measurement of energy distributions in ball mills. German Chemical Engineering Journal 7, 287–292.

Schonert, K., 1988. Fundamentals of Particle Breakage. Course notes. Section F6. Division of Continuing Engineering Education. University of the Witwatersrand, Johannesburg.

Vermeulen, L.A., 1985. The lifting action of lifter bars in rotary mills. Journal of South Africa Institute of Mining and Metallurgy 65 (2), 51–63.

Vermeulen, L.A., Howat, D.D., 1986. Fluctuations in the slip of grinding charge in rotary mills with smooth liners. International Journal of Mineral Processing 16, 153–168.

Vermeulen, L.E., Howat, D.D., 1988. Effects of lifter bars on the en-masse grinding media in milling. International Journal of Mineral Processing 24, 143–159.

Walton, O.R., Braun, R.L., 1993. Simulation of Rotary Drums and Repose Tests for Frictional Spheres and Rigid Sphere Clusters. Joint DOE/NSF Workshop on Flow of Particulates and Fluids. Ithaca, NY.

Watanabe, H., 1999. Critical rotation speed for ball-milling. Powder Technology 104, 95–99.

White, H.A., 1905. The Theory of the Tube Mill. The Journal of the Chemical, Metallurgical and Mining Society of South Africa, pp. 290–305.

Yashima, S., Hashimoto, H., Kanda, Y., Sano, S., 1988. Measurement of kinetic energy of grinding media in a tumbling ball mill. In: Forssberg, E. (Ed.), Proc. XVI Int. Min. Proces. Cong. Elsevier Science, Publishing, Amsterdam, pp. 299–309.